In discretising (17.2) finite difference expressions centred at grid point $(j+1/2, k)$ are used. This allows $\partial p/\partial x$ to be discretised as $(p_{j+1,k}-p_{j,k})/\Delta x$ which is a second-order discretisation about grid point $(j+1/2, k)$. Similarly (17.3) is discretised with finite difference expressions centred at grid point $(j, k+1/2)$ and $\partial p/\partial y$ is represented as $(p_{j,k+1}-p_{j,k})/\Delta y$.

The use of the staggered grid permits coupling of the u, v and p solutions at adjacent grid points. This in turn prevents the appearance of oscillatory solutions, particularly for p, that can occur if centred differences are used to discretise all derivatives on a non-staggered grid. The oscillatory solution is a manifestation of two separate pressure solutions associated with alternate grid points, which the use of centred differences on a non-staggered grid permits. The oscillatory behaviour is usually worse at high Reynolds number where the dissipative terms, which do introduce adjacent grid point coupling for u and v, are small. Clearly, from (17.1–3), there are no dissipative terms for p.

An additional advantage of a staggered grid is that the Poisson equation for the pressure (17.13) automatically satisfies the discrete form of the integral boundary condition (17.4). This avoids additional adjustments to the right-hand side of the Poisson equation, as is required in (16.98).

The use of staggered grids has some disadvantages. Computer programs based on staggered grids tend to be harder to interpret because it is desirable to associate a cluster of dependent variables with corresponding storage locations. Thus arrays storing u, v and p might associate storage location (j, k) with $u_{j+1/2,k}$, and $v_{j,k+1/2}$ and $p_{j,k}$ in Fig. 17.1. Generally boundary conditions are more difficult to impose consistently with a staggered grid, since at least one dependent variable, u or v, will not be defined on a particular boundary. If the grid is non-rectangular, and generalised coordinates (Chap. 12) are used, the incorporation of a staggered grid is more complicated.

The staggered grid shown in Fig. 17.1 is used in the MAC method (Sect. 17.1.2). In discretising (17.1–3) the following finite difference expressions are utilised:

$$\left[\frac{\partial u}{\partial t}\right]_{j+1/2,k} = \frac{(u^{n+1}_{j+1/2,k}-u^{n}_{j+1/2,k})}{\Delta t}+O(\Delta t)\ ,$$

$$\left[\frac{\partial u^2}{\partial x}\right]_{j+1/2,k} = \frac{(u^2_{j+1,k}-u^2_{j,k})}{\Delta x}+O(\Delta x^2)\ ,$$

$$\left[\frac{\partial (uv)}{\partial y}\right]_{j+1/2,k} = \frac{[(uv)_{j+1/2,k+1/2}-(uv)_{j+1/2,k-1/2}]}{\Delta y}+O(\Delta y^2)\ , \qquad (17.7)$$

$$\left[\frac{\partial^2 u}{\partial x^2}\right]_{j+1/2,k} = \frac{(u_{j+3/2,k}-2u_{j+1/2,k}+u_{j-1/2,k})}{\Delta x^2}+O(\Delta x^2)\ ,$$

$$\left[\frac{\partial^2 u}{\partial y^2}\right]_{j+1/2,k} = \frac{(u_{j+1/2,k-1}-2u_{j+1/2,k}+u_{j+1/2,k+1})}{\Delta y^2}+O(\Delta y^2)\ ,$$

$$\left[\frac{\partial p}{\partial x}\right]_{j+1/2,k} = \frac{(p_{j+1,k}-p_{j,k})}{\Delta x}+O(\Delta x^2)\ .$$

In the above expressions terms like $u_{j+1,k}$ appear, which are not defined in Fig. 17.1. To evaluate such terms averaging is employed, i.e.

$$u_{j+1,k}=0.5(u_{j+1/2,k}+u_{j+3/2,k})\ .$$

Similarly $(uv)_{j+1/2,k+1/2}$ is evaluated as

$$(uv)_{j+1/2,k+1/2}=[(u_{j+1/2,k}+u_{j+1/2,k+1})/2]\,[(v_{j+1,k+1/2}+v_{j,k+1/2})/2]\ .$$

17.1.2 MAC Formulation

One of the earliest, and most widely used, methods for solving (17.1–3) is the Marker and Cell (MAC) method due to Harlow and Welch (1965). The method is characterised by the use of a staggered grid (Sect. 17.1.1) and the solution of a Poisson equation for the pressure at every time-step. Although the original form of the MAC method has certain weaknesses, the use of a staggered grid and a Poisson equation for the pressure has been retained in many modern methods derived from the MAC method.

The method was developed initially for unsteady problems involving free surfaces. To allow the surface location to be determined as a function of time, markers (massless particles) are introduced into the flow. The markers are convected by the velocity field but play no role in determining the velocity or pressure fields. They will not be discussed further here. The impressive ability of the MAC formulation to give qualitatively correct simulations of complicated free-surface flows is illustrated in Fig. 17.2, which shows the time history of a drop falling into a stationary fluid.

In the MAC formulation the discretisations (17.7) allow the following explicit algorithm to be generated from (17.2 and 3):

$$u^{n+1}_{j+1/2,k}=F^{n}_{j+1/2,k}-\frac{\Delta t}{\Delta x}[p^{n+1}_{j+1,k}-p^{n+1}_{j,k}]\ , \qquad (17.8)$$

where

$$F^{n}_{j+1/2,k}=u^{n}_{j+1/2,k}+\Delta t\left[\frac{\{u_{j+3/2,k}-2u_{j+1/2,k}+u_{j-1/2,k}\}}{\mathrm{Re}\,\Delta x^2}\right.$$
$$+\frac{\{u_{j+1/2,k-1}-2u_{j+1/2,k}+u_{j+1/2,k+1}\}}{\mathrm{Re}\,\Delta y^2}-\frac{\{u^2_{j+1,k}-u^2_{j,k}\}}{\Delta x}$$
$$\left.-\frac{\{(uv)_{j+1/2,k+1/2}-(uv)_{j+1/2,k-1/2}\}}{\Delta y}\right]^{n}\ . \qquad (17.9)$$

Similarly the discretised form of (17.3) can be written as

$$v^{n+1}_{j,k+1/2}=G^{n}_{j,k+1/2}-\frac{\Delta t}{\Delta y}(p^{n+1}_{j,k+1}-p^{n+1}_{j,k})\ , \qquad (17.10)$$

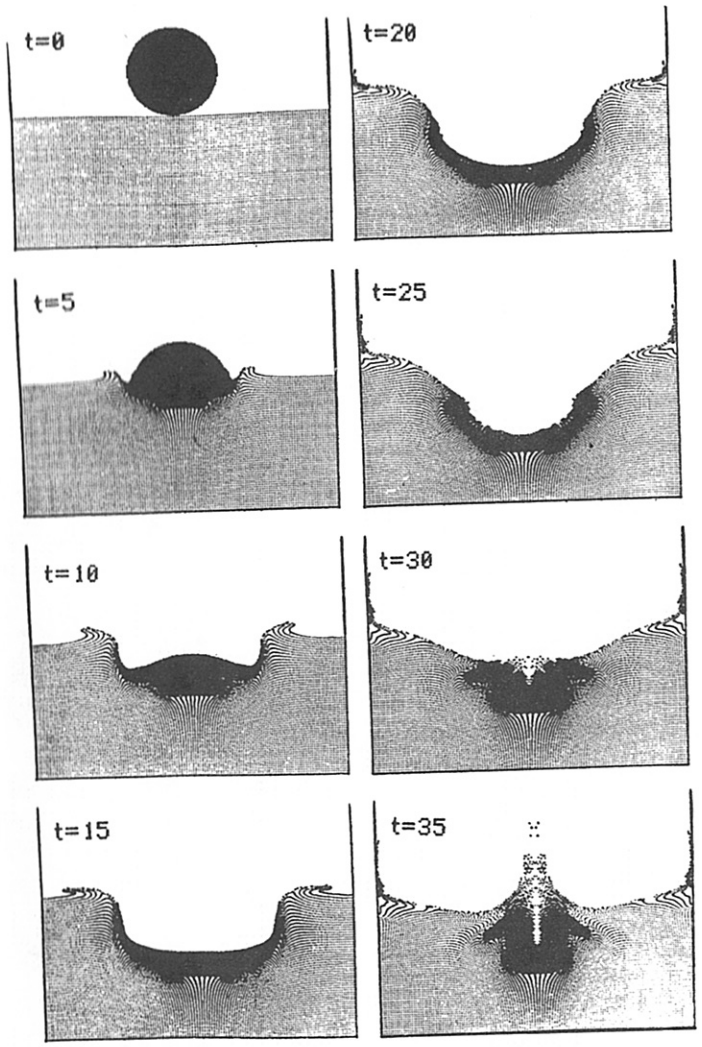

Fig. 17.2. Falling drop problem (after Harlow and Shannon, 1967; reprinted with permission of the American Association for the Advancement of Science)

where

$$G^n_{j,k+1/2}=v^n_{j,k+1/2}+\Delta t\left[\frac{\{v_{j+1,k+1/2}-2v_{j,k+1/2}+v_{j-1,k+1/2}\}}{\mathrm{Re}\,\Delta x^2}\right.$$
$$+\frac{\{v_{j,k+3/2}-2v_{j,k+1/2}+v_{j,k-1/2}\}}{\mathrm{Re}\,\Delta y^2}-\frac{\{(uv)_{j+1/2,k+1/2}-(uv)_{j-1/2,k+1/2}\}}{\Delta x}$$
$$\left.-\frac{\{v^2_{j,k+1}-v^2_{j,k}\}}{\Delta y}\right]^n . \qquad (17.11)$$

In (17.8 and 10) p appears implicitly; however, p^{n+1} is obtained before (17.8 and 10) are used, as follows. The continuity equation (17.1) is discretised as

$$D^{n+1}_{j,k}=\frac{(u^{n+1}_{j+1/2,k}-u^{n+1}_{j-1/2,k})}{\Delta x}+\frac{(v^{n+1}_{j,k+1/2}-v^{n+1}_{j,k-1/2})}{\Delta y}=0 , \qquad (17.12)$$

where $D_{j,k}$ is the dilatation for cell (j,k).

Substitution for $u^{n+1}_{j+1/2,k}$, etc., from (17.8 and 10) allows (17.12) to be rewritten as a discrete Poisson equation for the pressure, i.e.

$$\left[\frac{(p_{j-1,k}-2p_{j,k}+p_{j+1,k})}{\Delta x^2}+\frac{(p_{j,k-1}-2p_{j,k}+p_{j,k+1})}{\Delta y^2}\right]^{n+1}$$
$$=\frac{1}{\Delta t}\left[\frac{\{F^n_{j+1/2,k}-F^n_{j-1/2,k}\}}{\Delta x}+\frac{\{G^n_{j,k+1/2}-G^n_{j,k-1/2}\}}{\Delta y}\right] . \qquad (17.13)$$

If the various terms on the right-hand side of (17.13) are substituted from (17.9 and 11) the result can be written

$$\mathrm{RHS}_{(17.13)}=\frac{D^n_{j,k}}{\Delta t}-[L_{xx}\,u^2_{j,k}+2L_{xy}(uv)_{j,k}+L_{yy}\,v^2_{j,k}$$
$$-(1/\mathrm{Re}\{L_{xx}+L_{yy}\}D_{j,k}]^n , \quad \text{where} \qquad (17.14)$$
$$L_{xx}\,u^2_{j,k}=(u^2_{j-1,k}-2u^2_{j,k}+u^2_{j+1,k})/\Delta x^2 \quad \text{and}$$
$$L_{xy}(uv)_{j,k}=\{(uv)_{j+1/2,k+1/2}-(uv)_{j-1/2,k+1/2}-(uv)_{j+1/2,k-1/2}$$
$$+(uv)_{j-1/2,k-1/2}\}/\Delta x\Delta y .$$

In (17.14) $D^n_{j,k}/\Delta t$ may be interpreted as a discretisation of $-\partial D/\partial t|_{j,k}$ with $D^{n+1}_{j,k}=0$. Thus the converged pressure solution resulting from (17.13) is such as to cause the discrete form of the continuity equation to be satisfied at time level $n+1$.

Equation (17.13) is solved at each time-step, either using the iterative techniques described in Sect. 6.3 or the direct Poisson solvers described in Sect. 6.2.6. Once a solution for p^{n+1} has been obtained from (17.13), substitution into (17.8 and 10) permits $u^{n+1}_{j+1/2,k}$ and $v^{n+1}_{j,k+1/2}$ to be computed.

Since (17.8 and 10) are explicit algorithms for u^{n+1} and v^{n+1} there is a restriction on the maximum time step for a stable solution (Peyret and Taylor 1983, p. 148),

$$0.25(|u|+|v|)^2\,\Delta t\,\mathrm{Re}\leqq 1 \quad \text{and}$$
$$\Delta t/(\mathrm{Re}\,\Delta x^2)\leqq 0.25 , \quad \text{assuming that } \Delta x=\Delta y . \qquad (17.15)$$

Solution of (17.13) requires boundary conditions on p (Dirichlet) or, preferably, normal derivatives of p (Neumann) on all boundaries. For the flow over a backward-facing step (Fig. 17.14), it would be appropriate to impose Dirichlet boundary conditions on AF and AB and Neumann (normal) boundary conditions

on the walls FE, ED and DC. Typically the discretised form of the normal momentum equation is used to provide Neumann boundary conditions. For boundaries like FE, where the primary flow is parallel to the surface, the boundary layer assumption $\partial p/\partial n = 0$ can provide an appropriate Neumann boundary condition for p, if Re is large.

For internal flow problems Neumann (normal) boundary conditions are often prescribed for the pressure on all boundaries. In this case it is necessary that an additional global boundary condition be satisfied (as in Sect. 16.2.2). That is,

$$\iint\left(\frac{\partial^2 p}{\partial x^2}+\frac{\partial^2 p}{\partial y^2}\right)dx\,dy=\int_c \frac{\partial p}{\partial n}ds\ , \tag{17.16}$$

where the integral over c is made along the boundary of the computational domain. The left-hand side of (17.16) is evaluated in discrete form from the right-hand side of (17.13).

If the discrete form of (17.16) is applied with the MAC method to an internal cell, e.g. cell j, k in Fig. 17.1, it is satisfied exactly if $\partial p/\partial n$ on the right-hand side of (17.16) is evaluated from the normal momentum equation. If (17.16) is applied over the complete computational domain it is necessary that mass is conserved globally, i.e. (17.4) is satisfied, and that $\partial p/\partial n$ is evaluated on the boundary from the momentum equations in a manner consistent with the interior discretisation, or as $\partial p/\partial n = 0$, if appropriate.

Failure to satisfy the discrete form of (17.16) causes either very slow convergence of the solution of (17.13) or even divergence. Even when (17.16) is satisfied the occurrence of Neumann boundary conditions for the pressure leads to a slower convergence of the iteration than if all boundary conditions are of Dirichlet type.

However the use of Neumann boundary conditions for the pressure equation is recommended since the resulting solution is more likely to also be a solution of (17.1) to (17.3). An interesting discussion of the "correct" boundary conditions to be used with Poisson pressure equations is provided by Gresho and Sani (1987).

17.1.3 Implementation of Boundary Conditions

The grid is arranged so that boundaries pass through velocity points but not pressure points. For example, Fig. 17.3 shows the corner of a computational domain for which it is assumed that BC is a solid wall and AB is an inflow boundary.

Clearly $v_{1,1/2} = v_{2,1/2} = \ldots = 0$, since BC is a solid wall. Evaluation of (17.9) at node $(\frac{3}{2}, 1)$ requires knowledge of $u_{3/2,0}$. This can be obtained from the wall value,

$$u_{3/2,1/2} = 0 = 0.5(u_{3/2,1} + u_{3/2,0}) \quad \text{or} \quad u_{3/2,0} = -u_{3/2,1}\ .$$

On AB, u and v are given. The component u is used directly but $v_{1/2,k}$ is used to give a value to $v_{0,k}$. Thus in the evaluation of (17.11) at node $(1, \frac{3}{2})$, $v_{0,3/2}$ is given by

$$v_{0,3/2} = 2v_{1/2,3/2} - v_{1,3/2}\ .$$

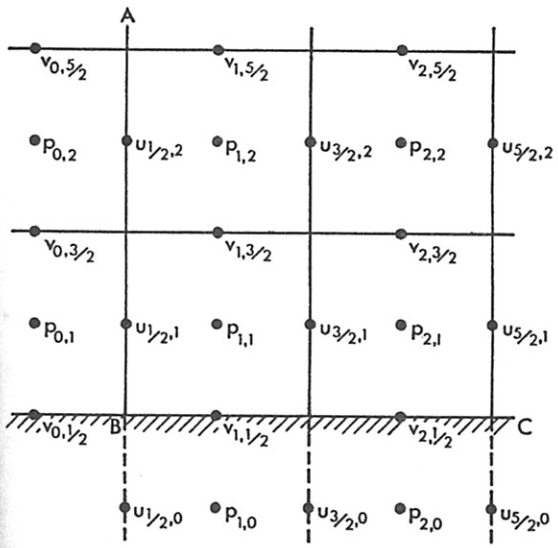

Fig. 17.3. Typical boundary orientation in relation to the staggered grid

If AB were an outflow boundary, with u positive, typical boundary conditions would be

$$\left.\frac{\partial u}{\partial x}\right|_{AB} = 0\ , \quad \left.\frac{\partial v}{\partial x}\right|_{AB} = 0\ . \tag{17.17}$$

If (17.9) is evaluated on AB at node $(\frac{1}{2}, 2)$, (17.17) would be used to set $u_{3/2,2} = u_{-1/2,2}$. Similarly in evaluating (17.11) at node $(0, \frac{3}{2})$, (17.17) would be used to set $v_{1,3/2} = v_{0,3/2}$.

The evaluation of the Poisson equation for the pressure (17.13) requires values of the pressure outside of the domain. When (17.13) is evaluated centred at node (2, 1) values of $p_{2,0}$ and $v_{2,-1/2}$ are required. $p_{2,0}$ is obtained by evaluating (17.3) centred at the wall, i.e. $\partial p/\partial y = (\partial^2 v/\partial y^2)/\mathrm{Re}$, since v at the boundary is not a function of time. In discretised form this becomes

$$\frac{p_{2,1}-p_{2,0}}{\Delta y} = \frac{1}{\mathrm{Re}}\frac{v_{2,3/2}-2v_{2,1/2}+v_{2,-1/2}}{\Delta y^2}\ .$$

To satisfy (17.1) at the wall, $\partial v/\partial y = 0$ so that $v_{2,-1/2} = v_{2,3/2}$ and

$$p_{2,0} = p_{2,1} - \frac{2v_{2,3/2}}{\mathrm{Re}\,\Delta y}$$

Harlow and Welch (1965) and Viecelli (1971) discuss appropriate boundary condition implementation at free surfaces.

17.1.4 Developments of the MAC Method

In the MAC method the pressure solution has the auxiliary task of satisfying continuity. A simplified Marker and Cell (SMAC) method has been developed by